Front. Phys. China (2006) 2: 204–208
DOI 10.1007/s 11467-006-0014-z

RESEARCH ARTICLE

**XIAO Jing-hua, LI Hai-hong, YANG Jun-zhong，
HU Gang**

Chaotic Turing pattern formation in spatiotemporal systems

Abstract The problem of Turing pattern formation has attracted much attention in nonlinear science as well as physics, chemistry and biology. So far spatially ordered Turing patterns have been observed in stationary and oscillatory media only. In this paper we find that spatially ordered Turing patterns exist in chaotic extended systems. And chaotic Turing patterns are strikingly rich and surprisingly beautiful with their space structures. These findings are in sharp contrast with the intuition of pseudo-randomness of chaos. The richness and beauty of the chaotic Turing patterns are attributed to a large variety of symmetry properties realized by various types of self-organizations of partial chaos synchronizations.

Keywords Turing pattern, spatiotemporal chaos, chaotic Turing pattern, chaos synchronization, self-organization, symmetry breaking

PACS Numbers 82.40.Ck, 05.45.Xt, 82.20.Wt

It has been known for a half of century since the pioneering work of Turing [1] that localized structures, namely Turing patterns, can appear from stationary homogeneous media by varying diffusion parameters [1–6]. Turing pattern formation has attracted great attention in nonlinear science as well as physics [2–5], chemistry [6–7] and biology [8]. A very recent and significant advance in this direction is that spatially ordered oscillatory Turing patterns were observed at the Turing instabilities of periodic homogeneous media [9–12]. On the other hand, in the past several decades, the issue of chaos in spatiotemporal systems has become one of the focuses in nonlinear science [13–16]. It seems very unlikely that chaotic systems could generate spatially ordered Turing patterns, because temporally chaotic motions (trajectories are sensitive to extremely small perturbations) are not supposed compatible with ordered space structures (which should be stable against rather strong noise). So far spatially disordered while localized chaotic Turing patterns were reported a decade ago in terms of phase separation of chaotic map lattices [17]; space orderings of chaotic patterns have been explored near the instability of synchronous chaos [18, 19]; and some symmetry properties of a few coupled chaotic oscillators have been investigated, based on the concept of partial synchronization [20–22]. However, the topic of spatially ordered Turing pattern formation in chaotic extended systems has not been systematically investigated.

In this work, we find that spatially ordered Turing patterns exist in chaotic extended systems. In addition, chaotic Turing patterns are strikingly rich and surprisingly beautiful with their space structures. The richness and beauty of the chaotic Turing patterns are due to a large variety of symmetry properties realized by various types of self-organizations of partial chaos synchronizations in the pattern formation.

In this paper, we study diffusively coupled Rossler systems in two-dimensional ($L\times L$) plane with periodic boundary condition and chaotic local dynamics

$$\begin{aligned}
&\partial_t u(x,y) = -(v+w) + D_u \nabla u \\
&\partial_t v(x,y) = u + Av + D_v \nabla v \\
&\partial_t w(x,y) = uw - Cw + B + D_w \nabla w \qquad (1) \\
&\nabla = \frac{\partial}{\partial x^2} + \frac{\partial}{\partial y^2} \\
&u,v,w(x+L,y) = u,v,w(x,y+L) = u,v,w(x,y)
\end{aligned}$$

Let us start our investigation from chaos synchronization. In Fig. 1(a) we show a critical curve above which the extended system is completely synchronous, i.e., all space

XIAO Jing-hua, LI Hai-hong, YANG Jun-zhong
School of Science, Beijing University of Posts and Telecommunications, Beijing 100876, China

HU Gang（✉）
Department of Physics, Beijing Normal University, Beijing 100875, China
E-mail：ganghu@bnu.edu.cn

Received March 24，2006

points of the medium follow an identical chaotic temporal orbit [see Fig.1(b)]. Below the threshold synchronous chaos becomes unstable, and various desynchronous and chaotic motions can be observed. In Fig. 1(c) we choose a parameter set below the threshold curve, the space-time waves look chaotic in both time and space. From Fig. 1(b) one can hardly imagine that the chaotic randomness can be associated with any finely ordered spatial structure.

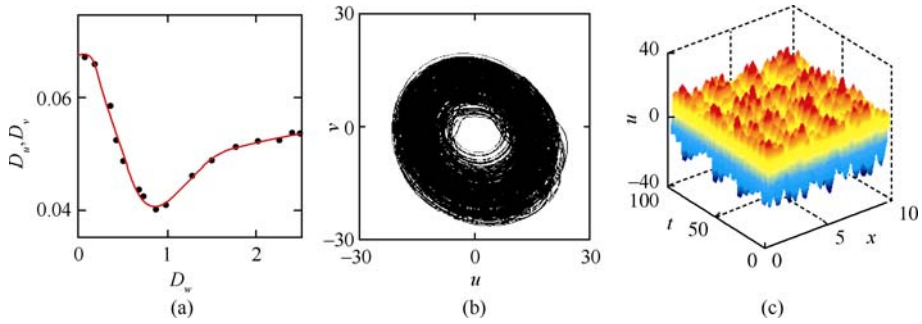

Fig. 1 Results of numerical simulations of Eq.(1) with A=0.2, B=0.2, C=4.5. 40×40 pixels are applied for discretization of 10×10 physical space. These parameters are used for all the figures unless specified otherwise. In simulations we start from the initial conditions $u(x, y, 0)=v(x, y, 0) =w(x, y,0)=\delta(x, y)$ with $\delta(x, y)$ being randomly chosen in [0.0, 0.2]. (**a**) Critical curve in the diffusion parameter plane ($D_u = D_v$) for the stability of synchronous chaos of Eq.(1). Chaotic Turing patterns can be observed below the threshold. (**b**) A chaotic trajectory of synchronous chaos of Eq.(1). (**c**) $D_u = D_v$ =0.005, D_w =2.5 (below the critical curve). Chaotic waves in (t, x) plane for y=4.

However, the spatial distributions of variables provide completely different pictures. In Figs. 2(a) – (c) we plot the snapshots of spatial distributions of variable $u(x, y, t)$ at different time instants with 40×40 pixels. The spatial contours show nicely ordered structures in sharp contrast with the chaotic waves of Fig. 1(c). It is clear from these contour figures that after desynchronization of homogeneous chaos the chaotic motions of different space points retain certain partial synchronizations, which provide some well organized spatial structures. There are a number of ordered patterns appearing in the time evolution. As time goes on, the system state varies from one pattern to another chaotically. And it is the chaoticity in pattern alternations that leads to the random-like trajectories of Fig. 1(c). In Fig. 2(a) –2(c) one can observe a characteristic wave length. When we enlarge the system size to 80×80 pixels with coupling unchanged, we find in Figs. 2(d)–2(f) the same wave length with the number of waves doubled.

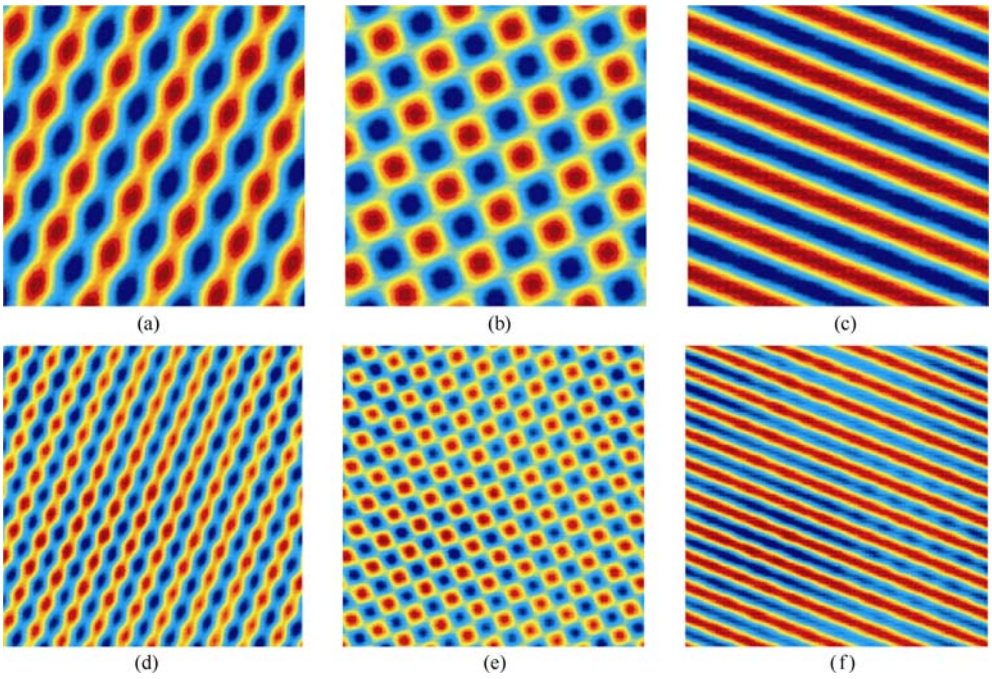

Fig. 2 Snapshots of contour pictures of the time evolution of $u(x, y, t)$ at different time instants. (**a**) – (**c**) Numerical results in 40×40 pixels (**a**) t =2 000.5 ; (**b**) t =2 001.8; (**c**) t =2 002.1. D_u , D_v and D_w are the same as Figs.1(**c**). (**d**) – (**f**) The same as (**a**) to (**c**) with 80×80 pixels in 20×20 physical plane used. (**a**) t=1 999.5;(**b**) t=2 000.8;(**f**) t=2 001.1.

The most important characteristic feature of Turing patterns is localization of space variable distributions. In order to test the existence of localized structures of the chaotic patterns we compute a distribution of $u_M(x,y)$ which is the maximum of $u(x,y,t)$ at the space point (x, y) over a long time interval T. And a number of distributions of $u_M(x,y)$ are plotted in Fig.3 for different sets of coupling

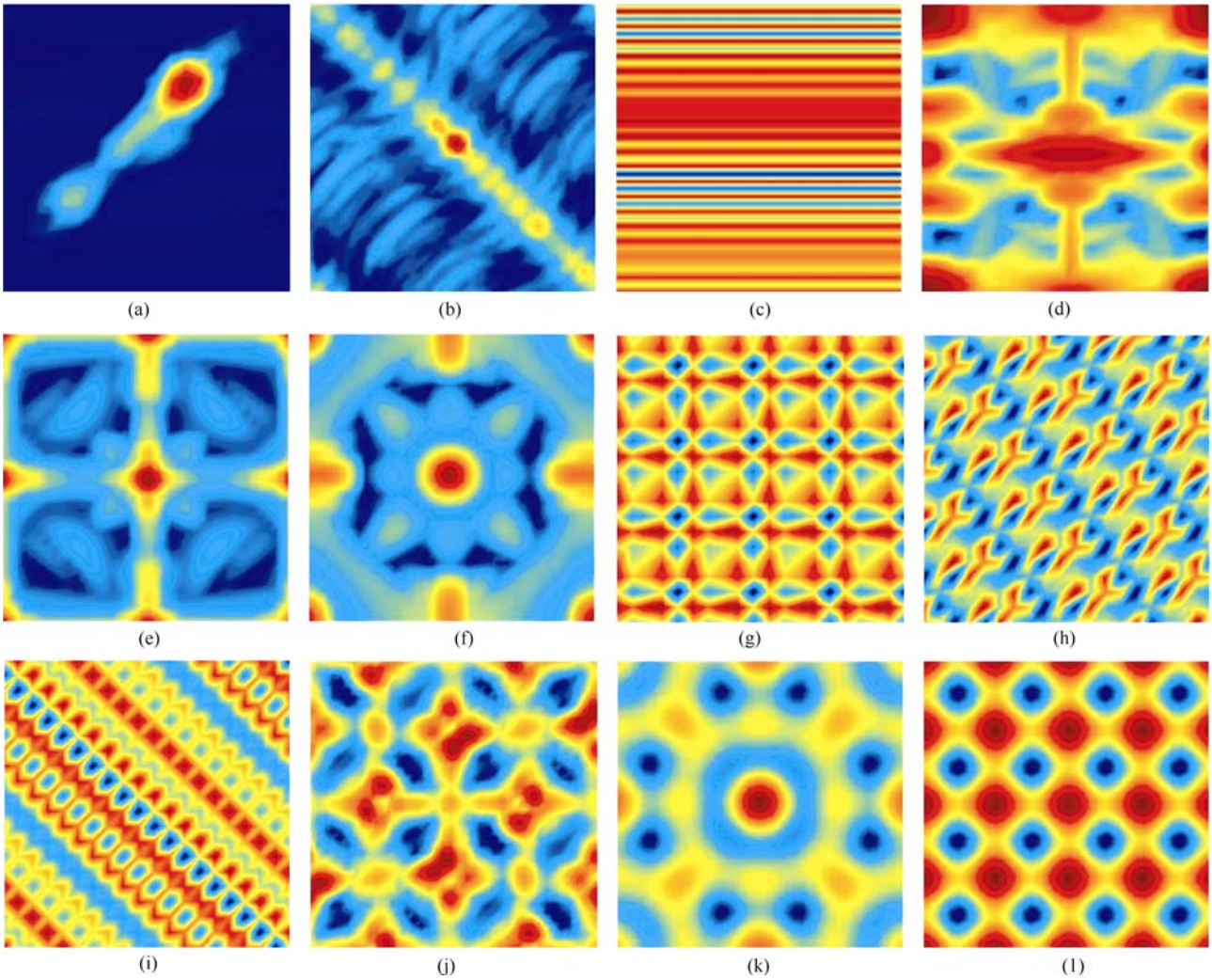

Fig.3 Beauty of chaotic Turing patterns. Contour pictures of $u_M(x,y)$ plotted for different coupling parameters where $u_M(x,y)$ is defined as the distribution of the maximum values of $u(x, y, t)$ over a time interval T=20 000 (about 3 000 circles of the Rossler oscillations). Localized Turing spots are observed without ambiguity. (**a**) $D_u = D_v$=0.017, D_w=1.25. Asymmetric Turing pattern. (**b**) $D_u = D_v$=0.015, D_w=0.65. Turing pattern with mirror reflection symmetry against a diagonal axis. (**c**) $D_u = D_v$=0.023, D_w=2.5. Turing pattern with continuous translational symmetry in x- direction. (**d**) , (**e**), (**f**) Spontaneous emergences of two reflection symmetry axes (x- and y- axes) and a symmetry center (0,0). (**d**) $D_u = D_v = D_w$=0.048. (**e**) $D_u = D_v$=0.045, D_w=0.25. (f) $D_u = D_v$=0.047, D_w=0.25. (**g**) , (**h**) , (**i**) Turing patterns invariant under different discrete translational transformation groups. (**g**) $D_u = D_v$=0.003, D_w=2.5. Translational symmetries $u_m(x+nL/4, y+mL/4) = u_M(x,y), n,m = \pm1,\pm2,\pm3$. (**h**) $D_u = D_v$=0.004, D_w=2.5. Translational symmetries $u_M(x+nL/5, y+nL/5) = u_M(x+mL/7, y-mL/6) = u_M(x,y), n,m = \pm1,\pm2,\cdots$. (**i**) $D_u = D_v$=0.01, D_w=2.5. Translational symmetries along a diagonal direction $u_M(x+nL/18, y-nL/18) = u_M(x,y), n = \pm1,\cdots,\pm17$. (**j**) $D_u = D_v$=0.024, D_w=2.5. Turing pattern with a symmetry center while without any mirror symmetry axis. (**k**) $D_u = D_v$=0.032, D_w=2.5. Turing pattern with rotational symmetries of π/2 and π rotation angles. (**l**) $D_u = D_v$=0.03, D_w=2.5. Turing pattern with all mirror reflective, translational and rotational symmetries.

parameters. Unlike the snapshots in Fig.2 showing explicit time variation of $u(x, y, t)$ patterns, the patterns of $u_M(x,y)$ in Fig.3 manifest the asymptotic distributions implicit in the long time statistics (note, further increase of length T does no longer change the contour pictures). Therefore, the figures in Fig.3 show the localized Turing spots in chaotic

media, which are called chaotic Turing patterns.

By varying coupling parameters, one can observe a large number of characteristically different chaotic Turing pictures. Some patterns of Fig.3 have not been observed in the conventional Turing patterns of stationary and periodic media. The conventional Turing patterns are determined strictly by one or few modes at instabilities, and these unstable modes produce some typical types of Turing patterns, e.g., hexagonal, squares, rolls, honeycombs, stripes, and their combinative and periodically alternative structures [9–10]. In contrast, in chaotic spatiotemporal systems, owing chaoticity, many modes can be easily coupled and involved in the pattern formation process, and this provides much larger freedom to generate a large variety of distinctive patterns. Note, all the figures in Fig.3 are observed in the same system of Eq.(1) with variations of the diffusion coefficients only.

In Fig.3, most of pictures have well organized structures rooted by different types of symmetry breakings. The synchronous state has full space symmetric properties, and thus does not have any spatial localization structure. The homogeneous distribution is invariant against all the space translation, mirror reflection, and rotation transformation groups. After the instability of the synchronous chaos most of these symmetries are broken, and the symmetries retained in the desynchronous chaos determine the spatial orderings of the inhomogeneous states and result in diverse structures.

In Fig. 3(a), the localized structure shows no symmetry, and it is a typical asymmetric Turing pattern (like a launching rocket). In Fig. 3(b) the state has the lowest symmetry, the mirror reflection symmetry against a diagonal axis $x + y$=0. The pattern of Fig. 3(c) possesses continuous translational symmetry in x-direction, i.e., $u_M(x+b,y) = (x,y)$ for arbitrary (x, y) and b. In Figs. 3(d)-3(f), the patterns are invariant against the mirror reflections with both x- and y- symmetry axes [$u_M(x,y) = u_M(x,-y) = u_M(-x,y]$= $u_M(-x,-y)$]. The spontaneous emergences of a symmetry center [set to (x, y)=(0,0) now] and two symmetry axes are the typical characteristics of these figures. Though all these three patterns possess the same symmetry properties, the pictures of (d) (sleeping-top-like), (e) (window-like) and (f) (flower-like) differ from each other considerably. Pattern Fig. 3(g) does not possess any mirror symmetry, but it has discrete translational symmetries along both x and y directions. And these symmetries yield a carpet-like pattern. Pattern Fig. 3(h) retains translational symmetries as well, but in two different directions. Figure 3(i) has both discrete translational and mirror reflective symmetries along a diagonal direction. It is interesting to see that this picture has 36 parallel and equivalent mirror symmetry axes, and these multiple symmetries make the picture resemble architecture, a beautiful chaotic architecture. The symmetry properties of Fig. 3(j) are different from all previous patterns. It has the translational symmetries of $u_M\left(x+nL/2, y+nL/2\right) = u_M\left(x+mL/2, y-mL/2\right) = u_M(x,y), n,m = \pm 1$ and the reflection symmetry against the symmetry center (0, 0), while it does not possess mirror symmetry against any axis. Figure 3(k) has mirror symmetries against four axis (x-, y-, x+y=0 and x–y=0 axes) and the rotational symmetries with π and $\pi/2$ angles against the rotation center (0, 0) (note, $\pi/2$ rotational symmetry does not exist in all the previous patterns). The pattern of Fig. 3(l) is similar most to the conventional Turing patterns. It possesses a large discrete symmetry group of all translational symmetries $u_M\left(x+nL/4, y+mL/4\right) = u_M(x,y), n,m = 0,1,2,3$,mirror reflection symmetries(with 8 horizontal and 8 vertical symmetry axes and 64 symmetry centers), and rotational symmetries of $\pi/2$ and π rotation angles against all the 64 symmetry centers.

Three points are crucial for characterizing chaotic Turing patters: (i) Chaoticity of temporal motions; (ii) Chaos synchronizations among partial space points; (iii) Space orderings organized by these partial chaos synchronizations. In Fig.4, we perform some standard numerical and statistical measurements to demonstrate these aspects. We show a divergence of adjacent trajectories in Fig. 4(a), indicating chaos without ambiguity. In Fig.4(b) we compute a modified correlation function [23] for different space pints

$$S(x,y) = \sqrt{\frac{\left\langle \left[u_{x_0,y_0}(t) - u_{x,y}(t) \right]^2 \right\rangle}{\left[\left\langle u^2_{x_0,y_0}(t) \right\rangle \left\langle u^2_{x,y}(t) \right\rangle \right]^{1/2}}} \qquad (2)$$

$$\left\langle f_{x,y} \right\rangle = \lim_{T\to\infty} \frac{1}{T} \int_0^T f_{x,y}(t)\mathrm{d}t$$

Function (2) is equivalent to standard space correlations, however, the form of Eq.(2) is particularly useful for quantitatively measuring the degree of chaos synchronization. In Fig.4(b), we observe $S(x,y) \approx 0$ in a number of space areas, identifying chaos synchronizations. A striking observation is that these synchronous space units are distantly away from each other and they are desynchronous from all the space sites around them, a typical feature of nonlocal chaos synchronization [24]. In Fig. 4(c), we plot the average absolute differences of space variables

$$\Delta(x,y) = \lim_{T\to\infty} \frac{1}{T} \int_0^T \left| u(x,y,t) - u(x_0,y_0,t) \right| \mathrm{d}t \qquad (3)$$

In Figs. 4(b) and (c) spatial orderings induced by perfect self-organization of chaos synchronization become apparent. These orderings are irrelevant to the position of the reference point (x_0, y_0). Note Figs. (1c), 4(b) and 4(c) represent the same spatiotemporal state. After a long time average, we explore strikingly well ordered space structure of Figs. 4(b) and (c) from the pseudo-random chaotic state Fig.1(c).

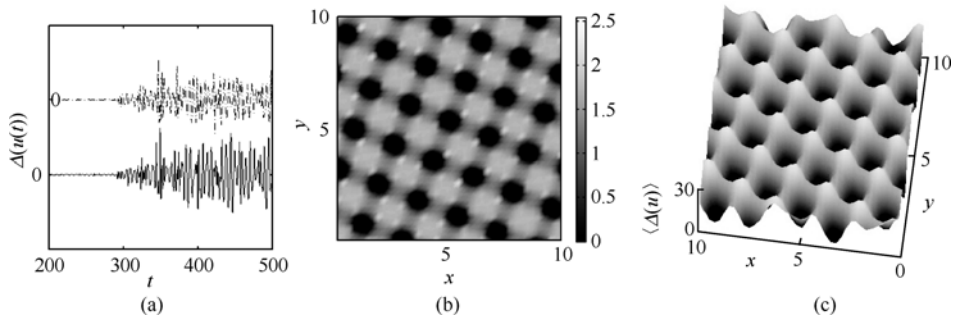

Fig.4 System parameters are the same as Fig. 2. (**a**) Divergence of two adjacent trajectories with exactly the same initial variables except a 10^{-3} deviation at a single site (5, 5). Real line shows the divergence of the two trajectories at site (5, 5), and dished line shows that at site (10, 10) with the largest distance from (5, 5). (**b**) Function $S(x, y)$ given by Eq.(2). (**c**) Average absolute difference given by Eq.(3). In (b) and (c) both $S \approx 0$ and $\Delta \approx 0$ represent partial chaos synchronizations.

In conclusion, we have revealed localized and spatially ordered structures of Turing patterns in chaotic extended systems. The richness and complexity of the chaotic Turing patterns are due to the diverse symmetry properties realized by partial chaos synchronizations. The present work focuses on the numerical demonstrations of Turing patterns in a single chaotic Rossler system with a specific coupling structure. We find similar phenomena in other systems, such as Rossler systems with different coupling structures and coupled Lorenz equations and Chua's circuit systems and so on. Further explorations of chaotic Turing patterns in natural pattern formation processes and in experimental realizations will stimulate a new area of pattern formation.

Acknowledgements This work was supported by the National Natural Science Foundation of China under Grant Nos. 10335010，10575016 and by Nonlinear Science Project.

References

1. TURING A.-M., The chemical basis of morphogenesis, Philos Trans. R. Soc. Landon, 1952, B237: 37–72
2. OUYANG Q. and SWINNEY H.-L., Transition from a uniform state to hexagnal and striped Turing patterns, Nature, 1991, 352: 610–612
3. CROSS M.-C. and HOHENBERG P.-C., Pattern-formation outside of equilibrium, Rev. Mod. Phys., 1993, 65: 851–1112
4. MIGUEZ D.-G., NICOLA E.-M., MUNUZURI A.-P., CASADEMUN J., SAGUES F., and KRAMER L., Traveling-Stripe Forcing Generates Hexagonal Patterns, Phys. Rev. Lett. 2004, 93: 048302
5. SCHMIDT B., KEPPER P.-D., and MULLER S.-C., Destabilization of Turing structures by electric fields Phys. Rev. Lett. 2003, 90: 118302
6. LI Y.-J., OSLONOVITCH J., MAZOUZ N., PLENGE F., KRISCHER K., and ERTL G., Turing-Type Patterns on Electrode Surfaces, Science, 2001, 291: 2395–2398
7. KURAMOTO Y., Chemical Oscillations, Waves and Turbulence, Springer-Verlag, Berlin, New York, 1984
8. MURRAY J.-D., Mathematical Biology, Springer-Verlag, Berlin, 1989
9. YANG L.-F., ZHABOTINSKY A.-M. and EPSTEIN I.-R., Stable squares and other oscillatory turing patterns in a reaction-diffusion model, Phys. Rev. Lett., 2004, 92: 198303
10. YANG L.-F., and EPSTEIN I.-R., Oscillatory Turing Patterns in Reaction-Diffusion Systems with Two Coupled Layers, Phys. Rev. Lett. 2003, 90:178303
11. WALGRAEF D., Spatio-Temporal Pattern Formation, Springer, New York, 1997
12. VANAG V.-K. and EPSTEIN I. R., Stationary and oscillatory localized patterns, and subcritical bifucations, Phys. Rev. Lett., 2004, 92:128301
13. EGOLF D.-A., MELNIKOV I., PESCH W. and ECKE R.-E., Mechanisms of extensive spatiotemporal chaos in Rayleigh-Bernard convection, Nature, 2000, 404: 733–736
14. GORYACHEV A., CHATE H., and KAPRAL R., Synchronization defects and broken symmetry in spiral waves, Phys. Rev. Lett. 1998, 80:873–876
15. CROSS, M.-C. and HOHENBERG, P.-C. Spatiotemporal chaos, Science, 1994, 263: 1569–1570
16. PANICONI M. and ELDER K.-R., Stationary, dynamical, and chaotic states of the two-dimensional damped Kuramoto-Sivashinsky equation, Phys. Rev. E，1997, 56, 2713–2721
17. RICARD V. and JORDI B., Chaotic Turing Structures, Phys. Lett. A, 1993, 179: 325–331
18. PECORA L.-M.，Synchronization conditions and desynchronizing patterns in coupled limit-cycle and chaotic systems, Phys. Rev. E., 1998, 58: 347–360
19. HU G., ZHANG Y., CERDEIRA H.-A., and CHEN S.-G., From low-dimensional synchronous chaos to high-dimensional desynchronous spatiotemporal chaos in coupled systems, Phys. Rev. Lett.，2000, 85: 3377–3380
20. WANG S.-H., XIAO J.-H, WANG X.-G., HU B.-B, and HU G., Spatial orders appearing at instabilities of synchronous chaos of spatiotemporal systems, Eur. Phys. J. B, 2002, 30: 571–575
21. RANGRAJIAN G.，CHEN Y.，and DING M.，Generalized Turing patterns and their selective realization in spatiotemporal systems, Phys. Lett. A 2003, 310:415–422
22. POGROMSKY A.，SANTOBONI G.，and NIJIMEIJER H.，Partial Synchronization: From Symmetry Towards Stability, Physica D, 2002, 172: 65–87
23. ROSENBLUM M.-G., PIKOVSKY A.-S., and KURTHS J., Phys.Rev.Lett. 1996, 76:1804–1807
24. ZHAN M., ZHENG Z.-G., HU G. and PENG X.-H, Nonlocal chaotic phase synchronization, Phys. Rev. E, 2000, 62: 3552–3557